

1 **Supplement for "Secondary organic aerosol**
2 **formation from idling gasoline passenger vehicle**
3 **emissions investigated in a smog chamber"**

4

5 **E. Z. Nordin¹, A. C. Eriksson², P. Roldin², P. T. Nilsson¹, J. E. Carlsson¹, M. K.**
6 **Kajos³, H. Hellén⁴, C. Wittbom², J. Rissler¹, J. Löndahl¹, E. Swietlicki², B.**
7 **Svenningsson², M. Bohgard¹, M. Kulmala^{2,3}, M. Hallquist⁵ and J. H. Pagels¹**

8

9 [1]{Ergonomics and Aerosol Technology, Lund University, P.O. Box 118, SE-221 00 Lund,
10 Sweden}

11 [2]{Division of Nuclear Physics, Lund University, P.O. Box 118, SE-221 00 Lund, Sweden}

12 [3]{Department of Physic, University of Helsinki, P.O. Box 64, FIN-00014 Helsinki,
13 Finland}

14 [4]{Finnish Meteorological Institute P.O. Box 503, FIN-00101 Helsinki, Finland}

15 [5]{Department of Chemistry, Atmospheric Science, University of Gothenburg, SE-412 96
16 Gothenburg, Sweden}

17 Correspondence to E. Z. Nordin (erik.nordin@design.lth.se)

18

19

20

21

22

23

24

25

26

27

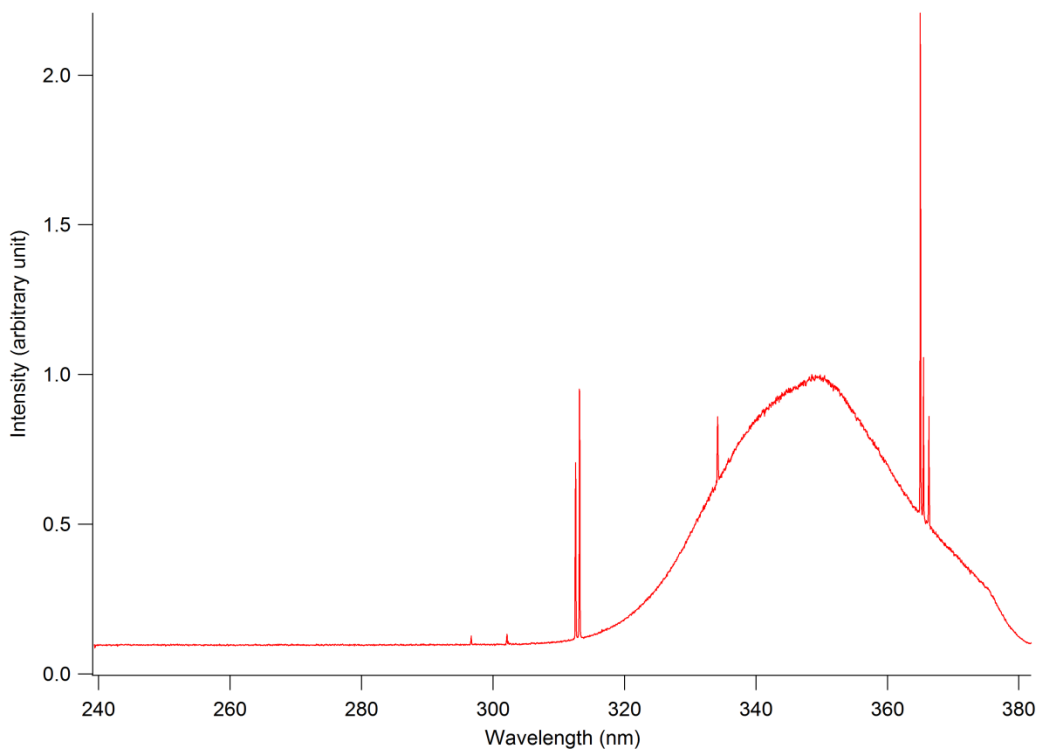
1 **Methods and material**

2 **Heated inlet system**

3 The raw exhaust was sampled from the exhaust pipe using a partial flow technique. The
4 sample was taken through a flexible stainless steel tube with a length of 1.5 m and an inner
5 diameter of 20 mm. The flexible tube was heated to 80 °C, which was higher than the exhaust
6 temperature (typically 70 °C). Downstream the ejector the diluted exhaust was transferred to
7 the smog chamber in a stainless steel pipe heated to 120 °C. The length of this pipe was 6 m
8 and the inner diameter was 10 mm.

9 **UV-spectrum**

10



11

12 Figure S1. The measured UV-intensity spectrum from the black-lights used in the smog
13 chamber.

14 **Cleaning of the Teflon chamber**

15 After a finished experiment the smog chamber was purged with filtered pressurized air. After
16 this the chamber was cleaned with >1 ppm ozone for at least 5 h. During the cleaning
17 procedure the UV-radiation was operated in 30 minute cycles without chamber cooling,

1 raising the smog chamber temperature to above 40 °C. This facilitates evaporation and
2 degradation of organic contaminants on the chamber walls. The chamber was finally purged
3 with dry pressurized air for several hours. Before each experiment, particle (AMS, SMPS)
4 and gas (NO_x, O₃ and PTR-MS (when available) phase instruments sampled from the smog
5 chamber to make sure that smog chamber was sufficiently clean. PTR-MS measurements
6 during the blank experiment show a total concentration of light aromatics of less than 1 ppb.

7 **Vehicles**

8 In total six gasoline passenger vehicles were tested at idling, the three cars selected
9 represented three different European emission classes. All tested vehicles used three way
10 catalysts. In the idling case, the cars were driven on a specified circuit until an engine
11 temperature of 55 ±5 °C was reached. In this case neither the engine nor the catalyst had
12 reached optimum operating temperature. Figure S2 shows the concentration of total-
13 hydrocarbons during a cold idling experiment (I3), measured with a flame ionization detector
14 (FID), calibrated with isobutene. In most experiments there was no systematic increase or
15 decrease in the THC levels in the exhaust with time.

16 Table S1. Technical data of the three gasoline light duty vehicles used

European emission standard class	Power (kW)	Odometer (km)	Displacement (cm ³)	Weight (kg)
EURO2	118	220 000	1948	1400
EURO3	115	180 000	1998	1426
EURO4	48	60 000	998	1050

17

18

19

20

21

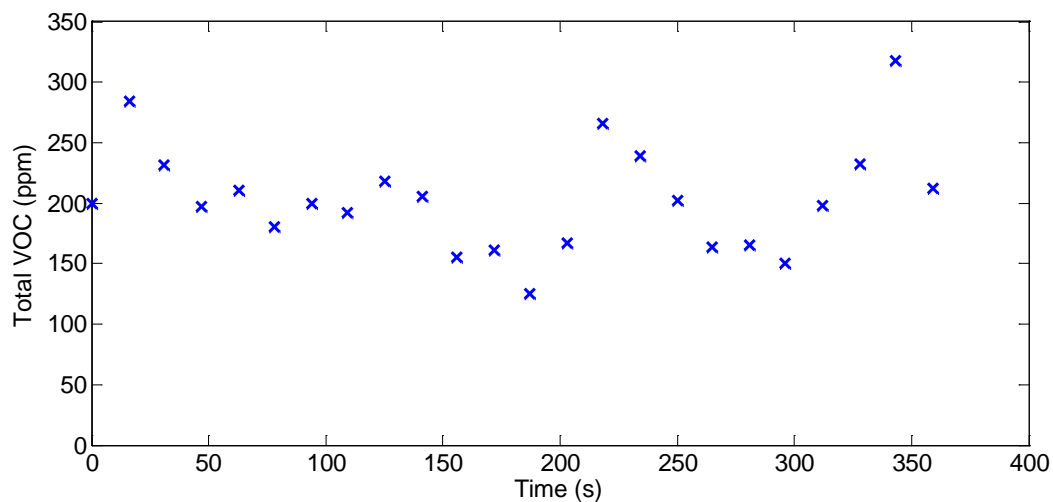
22

23

1 Table S2. Experimental conditions

Experiment	Total exhaust dilution	Ambient temperature °C
I1	31	-2
I2	109	-4
I3	90	-2
I4	78	-5
I5	27	3
S1	~1600	-5

2



3

4 Figure S2: The concentration of total hydrocarbons in the undiluted exhaust as a function of time,
5 experiment I3. The gasoline exhaust was added to the chamber for six minutes under idling conditions
6 from an initial engine temperature of 55 °C using the Euro 2 vehicle.

7 Experimental procedure

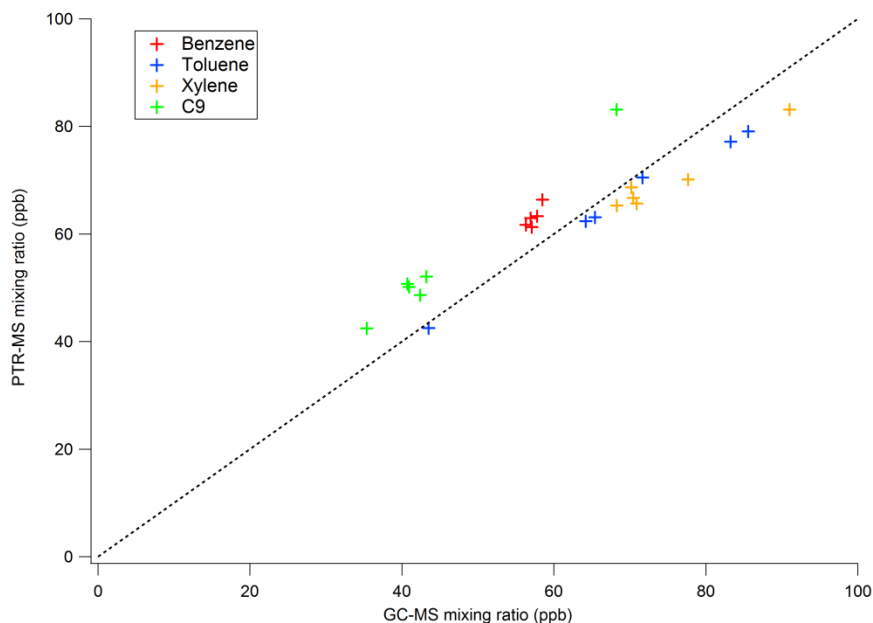
8 During the experiments the surrounding steel chamber was constantly flushed with pure air (5
9 air exchanges h⁻¹). To avoid leaks into the smog chamber from the surrounding steel room, an
10 overpressure was maintained in the smog chamber by manually elevating the floor and
11 lowering the roof of the smog chamber.

12 Results

13 Figure S2 shows a comparison between PTR-MS and GC-MS measurements. The average
14 ratio between the PTR-MS and GC-MS mixing ratio for each light aromatic is slightly lower

1 than 1 for toluene and xylenes, while it is higher for benzene and C₉ aromatics where the
2 latter has an average ratio of 1.2.

3



4

5 Figure S3. A comparison between PTR-MS and GC-MS for C₆-C₉ aromatics measured in the
6 smog chamber. The broken line shows a ratio of 1.

7 The PTR-MS method is based on reactions of hydronium ions (H₃O⁺) with gaseous
8 compounds having a larger proton affinity than that of H₂O, which results in a non-
9 dissociative proton transfer to a majority of the VOCs. The PTR-MS consists of a discharge
10 ion source to produce the primary ions, a drift-tube reactor, where the proton transfer reaction
11 between H₃O⁺ and the target VOC takes place and a quadrupole mass spectrometer for the
12 detection of reagent and product ions. Evidence of weak fragmentation of C₇ and C₈
13 compounds was found as suggested by a slightly larger ratio of PTR-MS to GC-MS for
14 benzene than for toluene and xylenes (Jobson et al., 2010).

15

16

17

18

19

1 Table S3. Chemical composition of the gasoline fuel and the undiluted gasoline exhaust.

Compound	Fuel (ng μg^{-1})	Exhaust ^a (mg m^{-3})
methyl tert-butyl ether (MTBE)	12.3	-
ethyl tert-butyl ether (ETBE)	0.5	-
benzene	11.7	13.96
toluene	117.9	16.02
ethylbenzene	19.0	2.83
p/m-xylene	72.2	14.49
o-xylene	21.1	5.90
propylbenzene	5.0	1.06
3-ethyltoluene	13.6	4.32
4-ethyltoluene	5.8	1.99
1,3,5-trimethylbenzene	6.8	2.42
2-ethyltoluene	4.6	1.76
1,2,4-trimethylbenzene	18.8	10.95
1,2,3-trimethylbenzene	3.2	1.72
2,2,4-trimethylpentane	112.4	1.14
hexane	68.3	2,13
heptane	20.7	2.67
octane	4.0	1.17
sulfur	<0.01	-
ethanol	5 vol%	-

2 ^aUndiluted concentrations, average for experiment I1-I3

3

4

5

6

7

8

9

10

1 Table S4. f_{43} and f_{44} fractions, reacted mass fractions and yield relative to m-xylene for the
 2 pure precursors presented in figure 8. These were used for calculations of the expected f_{43}
 3 and f_{44} of gasoline exhaust assuming that all SOA originated from C₆-C₉ light aromatic
 4 compounds.

Compound	f_{43}	f_{44}	Reacted mass fraction of (C ₆ -C ₉) LA (average of I1 and I2)	Reference
benzene	0.03	0.12	0.011	Ng et al., 2010
toluene	0.130	0.120	0.115	Chhabra et al., 2011
ethylbenzene	0.023	0.122	0.016	Sato et al., 2010
m/o/p-xylene	0.170	0.095	0.344 ^a	Exp. P2 this study
1,3,5-trimethylbenzene	0.175	0.055	0.100	Ng et al., 2010
1,2,4-trimethylbenzene	0.197	0.088	0.230	Derived from experiment P1
1,2,3-trimethylbenzene	0.197	0.088	0.047	Assumed to be same as 1,2,4-tmb
2/3/4-ethyltoluene and propyl benzene	0.110	0.105	0.137	Assumed as the mean of ethylbenzene and 1,2,4-trimethylbenzene
naphthalene ^b	0.01	0.1	-	Chhabra et al., 2011

5 ^aAll xylenes are assumed to have the same f_{43} and f_{44} as measured for m-xylene in exp. P2.

6 ^bNot included in calculation, given here for reference.

7 **Expected f_{43} and f_{44} assuming additive SOA composition and yield for C₆-C₉ Light** 8 **aromatics**

9 First we note that the f_{43} and f_{44} fractions for m-xylene in experiment P2 were within 0.02
 10 of values from several studies in the literature (Ng et al. 2010, Chhabra et al. 2011, Loza et al.
 11 2012) suggesting that these measurements are typically repeatable between instruments and
 12 set-ups. In Table S4 we list literature values for the most important C₆-C₉ light aromatic
 13 precursors, for compounds with no available literature data we had to make assumptions
 14 based on the structure of the component. For example, the three xylene isomers were assumed
 15 to have the same f_{43} and f_{44} fractions as found for m-xylene. This is supported by a study

1 with the potential aerosol mass chamber which showed that the f_{43} and f_{44} fractions of SOA
 2 from p- and m- xylene varied by less than 0.01 (Kang et al. 2011). The f_{43} and f_{44} values for
 3 1,2,4-trimethylbenzene were derived from experiment P1 (precursor mixture of 1,2,4 TMB,
 4 m-xylene and toluene), where 1,2,4 TMB constituted more than 60% of the reacted light
 5 aromatics. We used the f_{43} , f_{44} and yields for toluene and m-xylene given in Table S4 and
 6 assumed that the mixed SOA was additive in terms of yield and composition.

7 Finally, we estimated the expected f_{43} , f_{44} in each gasoline exhaust experiment if assuming
 8 additive yield and composition. The SOA contribution from each component was first
 9 calculated from the reacted mass fraction and yield using the high and low yield aromatic
 10 classes from Odum et al. (1997). Then the f_{43} and f_{44} fractions were calculated as the
 11 weighted sum of the thirteen different components in table S4. The resulting “expected” f_{43}
 12 and f_{44} are given in table S5.

13 Table S5. The expected and measured f_{43} and f_{44} for the six gasoline exhaust experiments.
 14 The expected f_{43} and f_{44} figures are based on the assumption that the SOA was produced
 15 only from light aromatics (C₆-C₉) and that the mass spectra of the gasoline exhaust can be
 16 calculated as the weighted mean of the SOA from each precursor. The f_{43} and f_{44} figures for
 17 13 pure C₆-C₉ light aromatic precursors (table S4) are used together with the GC-MS data of
 18 the reacted concentration for those precursors to calculate the expected f_{43} and f_{44} . Benzene,
 19 toluene, ethyl-benzene, propyl benzene and the ethyl-toluenes were assumed to have twice as
 20 high yield as m-xylene (Odum et al., 1997).

Exp.	Expected f_{43}	Expected f_{44}	Measured ^a f_{43}	Measured ^a f_{44}	Maximum fraction of C ₆ -C ₉ contribution to SOA ^b
I1	0.145	0.099	0.088	0.114	0.61
I2	0.148	0.097	0.090	0.130	0.61
I3	0.158	0.093	0.086	0.090	0.54
I4	0.138	0.103	0.080	0.130	0.58
I5	0.157	0.097	0.081	0.107	0.52
S1	0.142	0.101	0.148	0.095	1.04

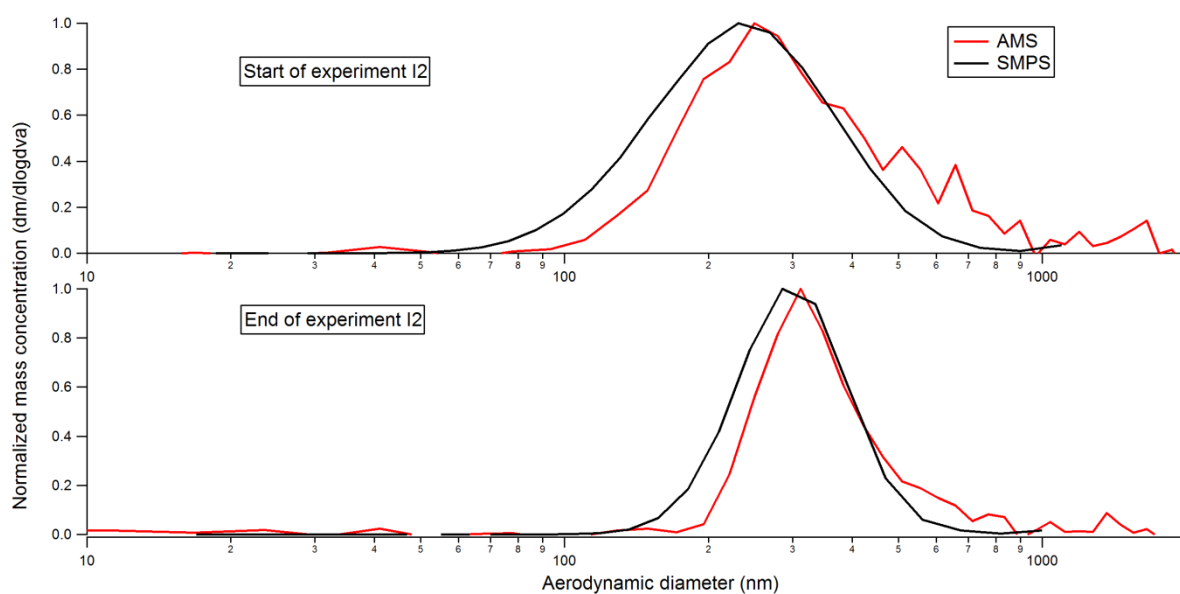
21 ^aPOA subtracted

22 ^bBased on the ratio between the measured and expected f_{43} .

1 Table S6. Estimations of potential SOA formed from C₁₀, C₁₁ light aromatics and
 2 naphthalene. For C₁₀ light aromatics, the reacted concentration was estimated from PTR-MS
 3 measurements. For C₁₁ light aromatics and naphthalene the initial concentration was first
 4 estimated using PTR-MS and the reacted concentration was calculated using $k_{OH} = 5.67 \cdot 10^{-11}$
 5 (C₁₁) and $k_{OH} = 2.44 \cdot 10^{-11}$ (naphthalene) (The Master Chemical Mechanism). The yield
 6 curves for C₁₀ and C₁₁ were assumed to be identical to m-xylene (according to the fit in figure
 7 5), while the yield for naphthalene is assumed to be three times the yield for m-xylene.

Exp. Id	Initial concentration of C ₁₀ / C ₁₁ / naphthalene (ppb)	Reacted conc. C ₁₀ / C ₁₁ / naphthalene ($\mu\text{g m}^{-3}$)	Estimated formed SOA C ₁₀ / C ₁₁ / naphthalene ($\mu\text{g m}^{-3}$)
I1	13.4/1.1/2.8	30.7/2.6/3.6	2.5/0.2/0.9
I2	17.7/1.6/4.4	40.1/5.9/6.0	4.6/0.7/2.1
S1	4.4/0.2/0.2	12.6/0.4/0.2	0.8/<0.1/<0.1

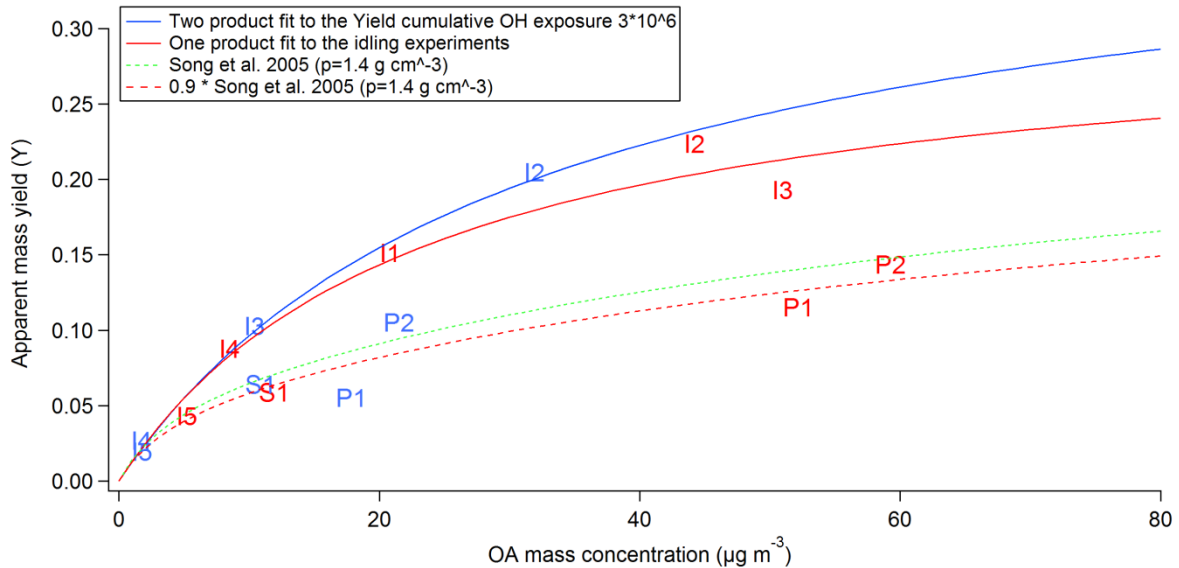
8
9
10



11
12 Figure S4. The normalized mass size distribution for SMPS and AMS at the start (before UV
 13 lights) and end of experiment I2. The SMPS volume size distribution is converted to mass
 14 size distribution by multiplying the volume with the density of the mixture calculated from

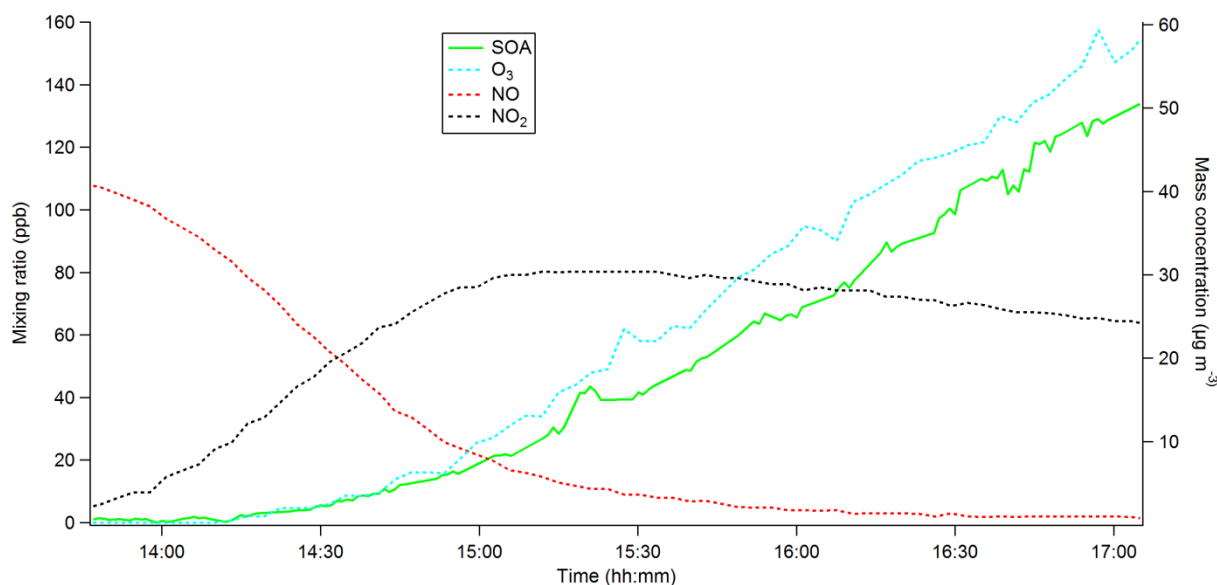
1 the AMS-data. The SMPS mobility diameter size channels have been converted to vacuum
2 aerodynamic diameters also using the density of the mixture.

3



4

5 Figure S5. The apparent mass yield for the gasoline exhaust and precursor experiment, end of
6 each experiment (red symbols) and at a cumulative OH exposure of $3 * 10^6 \text{ cm}^{-3} \text{ h}$ (blue
7 symbols). A one product fit (red solid line) is applied to the yield data at the end of the idling
8 experiments (same as figure 5 in the main paper). A two product fit is applied to the yield data
9 at cumulative OH exposure of $3 * 10^6 \text{ cm}^{-3} \text{ h}$ (blue solid line) the fitting parameters is
10 $a_1=0.3799$, $a_2=0.048$, $k_1=0.0332$ and $k_2= 0.0035$. The green and red broken lines are a two
11 product fit to the m-xylene yield from Song et al. (2005), (assuming a SOA density of 1.4 g
12 cm^{-3}).



1

2 Figure S6. Ozone, NO, NO₂ concentrations together with the wall loss corrected SOA mass
 3 concentration as a function of time in experiment I3. The data shows evidence of SOA
 4 production in the presence of NO, in contrast to the precursor experiments (e.g. Fig 3). UV-
 5 lights were turned on at 13:42.

6 References

7 Chhabra, P. S., Ng, N. L., Canagaratna, M. R., Corrigan, A. L., Russell, L. M., Worsnop, D.
 8 R., Flagan, R. C. and Seinfeld, J. H. (2011). *Elemental composition and oxidation of*
 9 *chamber organic aerosol*. *Atmos Chem Phys* **11**(17): 8827-8845.

10

11 Jobson, B. T., Volkamer, R. A., Velasco, E., Allwine, G., Westberg, H., Lamb, B. K.,
 12 Alexander, M. L., Berkowitz, C. M. and Molina, L. T. (2010). *Comparison of*
 13 *aromatic hydrocarbon measurements made by PTR-MS, DOAS and GC-FID during*
 14 *the MCMA 2003 Field Experiment*. *Atmos Chem Phys* **10**(4): 1989-2005.

15 Kang, E., Toohey, D. W. and Brune, W. H. (2011). *Dependence of SOA oxidation on organic*
 16 *aerosol mass concentration and OH exposure: experimental PAM chamber studies*.
 17 *Atmos Chem Phys* **11**(4): 1837-1852.

18

19 Loza, C. L., Chhabra, P. S., Yee, L. D., Craven, J. S., Flagan, R. C. and Seinfeld, J. H. (2012).
 20 *Chemical aging of m-xylene secondary organic aerosol: laboratory chamber study*.
 21 *Atmos Chem Phys* **12**(1): 151-167.

22

23 Ng, N. L., Canagaratna, M. R., Zhang, Q., Jimenez, J. L., Tian, J., Ulbrich, I. M., Kroll, J. H.,
 24 Docherty, K. S., Chhabra, P. S., Bahreini, R., Murphy, S. M., Seinfeld, J. H.,
 25 Hildebrandt, L., Donahue, N. M., DeCarlo, P. F., Lanz, V. A., Prevot, A. S. H., Dinar,
 26 E., Rudich, Y. and Worsnop, D. R. (2010). *Organic aerosol components observed in*

- 1 *Northern Hemispheric datasets from Aerosol Mass Spectrometry.* Atmos Chem Phys
2 **10**(10): 4625-4641.
- 3
- 4 Odum, J. R., Jungkamp, T. P. W., Griffin, R. J., Forstner, H. J. L., Flagan, R. C. and Seinfeld,
5 J. H. (1997). *Aromatics, reformulated gasoline, and atmospheric organic aerosol*
6 *formation.* Environ Sci Technol **31**(7): 1890-1897.
- 7
- 8 Sato, K., Takami, A., Isozaki, T., Hikida, T., Shimono, A. and Imamura, T. (2010). *Mass*
9 *spectrometric study of secondary organic aerosol formed from the photo-oxidation of*
10 *aromatic hydrocarbons.* Atmos Environ **44**(8): 1080-1087.
- 11 Song, C., Na, K. S. and Cocker, D. R. (2005). *Impact of the hydrocarbon to NO_x ratio on*
12 *secondary organic aerosol formation.* Environ Sci Technol **39**(9): 3143-3149.
- 13 The Master Chemical Mechanism: <http://mcm.leeds.ac.uk/MCM/>, last access: 13th November
14 2012